Theoretical Interpretation of the Fragments Generated from a Glycine Radical Cation

Hsiu-Feng Lu,*,† Feng-Yin Li,*, ‡ and S. H. Lin†

The Institute of Atomic and Molecular Sciences, Academia Sinica, P.O. Box 23−166, Taipei, Taiwan 106, R.O.C., and Department of Applied Chemistry, National Chi Nan Univerisity, 1 University Rd, Puli, Nantou, Taiwan, 545 R.O.C.

Received: May 28, 2004

By applying the CCSD(T)//B3LYP method with 6-31+G(d,p) basis sets, this work presents possible mechanisms of various fragmentation products found in the glycine mass spectrum. Imposing the criterion of low fragmentation energy enabled the *m*/*z* 17, 28, 29, 30, 31, 39, 41, 44, 45, and 74 fragments to be identified as NH_3^+, $HNCH^+$, H_2NCH^+, $H_2NCH_2^+$, $H_3NCH_2^+$, $NCCH^+$, H_2NCCH^+, NH_2CO^+, $COOH^+$, and $CH_2CO_2H^+$, respectively. This result indicates that the dominant fragmentation process arises from a $C_\alpha-C$ cleavage by abstracting COOH, which corresponds to the *m*/*z* 30 peak ($NH_2CH_2^+$). This interpretation is consistent with experimental observations. The neutral species ofthe *m*/*z* 28 ($HCNH^+$) peak is $CH(OH)_2$ rather than [CHO + H_2O] because the corresponding critical energy of the latter is higher than that of the former. The intermediates in the reaction pathway by which $NCCH^+$ and $HNCH^+$ fragments are formed reveal that water may participate in the reaction and stabilize the intermediates.

1. Introduction

The past decade has seen a rapid increase in interest in oxidative damage to proteins, and its relevance to pathological disorders and aging.[1] Although oxidation can have drastic effects on proteins as a whole, the most important reactions occur in the amino acids. A detailed investigation of the properties of amino acid and peptide radicals should be performed to understand the mechanism of the formation of this damage. Apart from its theoretical tractability, radicals derived from glycine have attracted much interest,[2−26] especially in relation to biology; for example, glycine residues are common in proteins with a substantial β sheet, such as silk fibroins. Because glycine has the second $^{\alpha}C-H$ bond that is exposed, it is susceptible to oxidative damage. Moreover, among residues in an antiparallel β sheet, only glycine is susceptible to damage by weak oxidants such as thiyl radicals and superoxide.[10] Another example is that one of the products of radiating glycine in solution or the stable glycyl cation $[NH_2CHCOOH]^+$ can be obtained by the dissociating ionization of various amino acids.[2] Hence, glycine radicals can serve as a model for predicting the probable reactions of the other amino acid and peptide radicals. In addition, the glycyl radical have some effects in *Escherichia coli* pyruvate formate lyase (PFL),[27,28] *E. coli* anaerobic RNR,[29−31] and bacteriophage T4 anaerobic RNR.[32,33] For example, in PFL, the glycyl radical catalyses the entire reaction mechanism of the cleavage of pyruvate to form formate and acetyl-CoA, which are subsequently used in the Krebs cycle.[27]

Studies of glycine radicals have concentrated on the C-centered glycyl radical $[NH_2CHCOOH]$[2−10] and protonated glycine,[10−18] and some studies have addressed the glycine radical cation $[NH_2CH_2COOH]^+$.[19−26] The latter can be considered to be a precursor of variously derived radicals. Two isomers of glycine radical cation exist, the keto and enol forms, and the threshold energy of the tautomerization between these two forms is substantial, disabling facile interconversion.[19] It is well known that the glycine radical cation in its enol form is thermodynamically more stable than in its keto form and that Marino et al. used the enol cation radical as starting species to study the potential energy surface.[24] The keto and enol forms of glycine radical cation can be generated by direct electron ionization (EI) of glycine and dissociative EI of isoleucine (McLafferty rearrangement), respectively.[23] The experimental observation[23] indicates that the bond cleavage behavior of the glycine radical cation in enol form is different from that in keto form, for example, the main peak of the metastable ion (MI) and collisionally activated dissociation (CAD) spectra of the glycine radical cation and the corresponding enol radical cation are *m*/*z* 30 and 57, respectively. The fragment of *m*/*z* 30, considered to be immonium $CH_2NH_2^+$, is also found in the experimental study.[20] Besides the main peak *m*/*z* 30, the femtosecond photoionization mass spectra[20] of ion-desorbed glycine also detected *m*/*z* 17, 24, 27, 28, 29, 31, 39, 41, 44, and 74, and the CAD and neutralization−reionization (NR) spectra[23] of the glycine radical cation both detected the signals of *m*/*z* 17, 28, 29, 30, 45, and 57 but with different fragment ion abundances and two additional peaks at 44 and 74 in the latter spectrum. The fragmentation of the enol form of the glycine radical cation has been suggested to form H_2O and aminoketene radical cation $[NH_2-HCCO]^+$; its reaction mechanism has been studied by Marino and Russo.[24] There are several theoretical studies related to the glycine radical cation in the keto form appearing in the literature recently. Simon et al.[25] calculated several fragmentation reactions of a glycine radical cation by breaking the C_α bond and found the abstractions of COOH, H, and NH_2 are easier that those of $COOH^+$, H^+, and NH_2^+, respectively. As an extension to the above study, our previous work located the related transition states with the corresponding activation energies for the fragmentation reactions of the C_α bond breaking from the glycine radical cation.[26] Both Simon et al.[24] and our pervious work[26] found that the dominate fragment is the

* Corresponding authors. E-mail: hflu@pub.iams.sinica.edu.tw (H.-F. L.) and feng64@ncnu.edu.tw (F.-Y. L).
† Academia Sinica.
‡ National Chi Nan Univerisity.

10.1021/jp047687k CCC: $27.50
Published on Web 09/29/2004

TABLE 1: Fragmentation Energies of Glycine Radical Cation at the CCSD(T)//B3LYP Level (in kcal/mol) Including the Zero Point Energy

reactions	6-31++G(d,p)[a]	6-31+G(d,p)[b]
$NH_2CH_2COOH^+ \rightarrow NH_2+CH_2COOH^+$	73.6	73.6
$NH_2CH_2COOH^+ \rightarrow H+NH_2CHCOOH^+$	27.1	27.4
$NH_2CH_2COOH^+ \rightarrow COOH+CH_2NH_2^+$	62.3	62.3
$NH_2CH_2COOH^+ \rightarrow COOH+CH_2NH_2^+$	16.1	16.0

[a] Values taken from Figure 3 of ref 25 with the zero point energy corrected. [b] Values obtained herein.

immonium ion $CH_2NH_2^+$ by abstracting the COOH, which is consist with the experimental results.[20,23] Rodriguez-Santiago et al.[22] focused only on fragmentation reaction pathways involving intramolecular proton transfers. In this study, we tried to cover the more probable fragmentation channels found in experimental studies[20,24] to understand the plausible fragmentation reaction mechanisms of the glycine radical cation in the keto form.

2. Methods

All molecular geometries and harmonic vibrational frequencies, including those of various glycine cation conformers, transition states, and fragments, are herein obtained using the (U)B3LYP method with 6-31+G(d,p) basis sets. With either 6-31+G(d,p) or 6-31++G(d,p) and 6-311+G(d,p) basis sets, the structural parameters of the resulting molecular geometries are very similar to corresponding glycine radical cation conformers of previously obtained theoretical values.[24,25,34] This implies that the 6-31+G(d,p) basis sets are sufficient to determine the optimized molecular geometries without the use of diffuse functions for hydrogen or the use of triple-ζ valence representation on all atoms. Rodriguez-Santiago et al.[22] found that the B3LYP method failed to estimate the relative energy between conformer **II(+)** and **V(+)** of the glycine radical cation and their intramolecular proton-transfer energy barrier when compared with results done with CCSD(T). Thus, several fragmentation energies of the glycine radical cation, obtained by the CCSD(T)//B3LYP method, including the zero point energy, are highly consistent with those found in ref 25, as indicated in Table 1. Therefore, to obtain the reaction energies and the corresponding energy barriers of the fragmentation reactions, we employed CCSD(T)//B3LYP with 6-31+G(d,p) basis sets. All calculations were performed using the Gaussian 98 package.[35]

The general procedure of this study is as follows. First, all possible cation radicals and their relative neutral counterparts were considered according to the *m*/*z* values, and then their structures were optimized, separately. The low fragmentation energy criterion was applied to identify the fragmentation radicals in the mass spectrum of the glycine radical cation. The corresponding mechanisms of fragmentation reactions were then investigated by searching the potential energy surfaces for the reaction-activated complexes, for example, possible candidates of *m*/*z* 30 cations are CH_3NH^+, $CHNH_3^+$, and $CH_2NH_2^+$. The results indicate that $CH_2NH_2^+$, with COOH as its neutral partner, is more stable than the other two cations, CH_3NH^+ and $CHNH_3^+$, whose energies relative to that of $CH_2NH_2^+$ are 95.1 and 98.4 kcal/mol, respectively, calculated by the B3LYP/6-31+G** method without ZPVE correction. Usually, the generation of fragments requires a multistep reaction, in which intermediates are involved before they dissociate. Sometimes the mechanism is determined backward, that is, from products, to find possible fragmentation precursors.

3. Results and Discussion

The mass spectrum of the glycine radical cation in the keto form shows that the $CH_2NH_2^+$ (*m*/*z* 30) cation was the major fragment ion, with minor amounts of the several cations such as *m*/*z* of 17, 24, 27, 28, 29, 31, 39, 41, 44, and 74.[20] The criterion of low formation energy was applied to determine that the *m*/*z* 17, 28, 29, 30, 31, 39, 41, and 44 peaks correspond to NH_3^+, $HNCH^+$, H_2NCH^+, $H_2NCH_2^+$, $H_3NCH_2^+$, $NCCH^+$, H_2NCCH^+, and NH_2CO^+, respectively. We failed to find the reaction mechanisms of *m*/*z* 24 and 27 with low fragmentation energy; however, the *m*/*z* 45, which is suggested to be the COOH cation, has been observed in the CAD, neutral fragment reionization (N_fR), and NR spectra.[23] Therefore, we investigated the reaction mechanisms generating various fragment cations such as NH_3^+, $HNCH^+$, H_2NCH^+, $H_2NCH_2^+$, $H_3NCH_2^+$, $NCCH^+$, H_2NCCH^+, NH_2CO^+, and $COOH^+$ from the glycine cation radical in the keto form along with their relationship to the energy profiles at the same time. The critical energy is defined as the minimum energy needed to observe the particular fragmentation, as described in ref 16.

3.1 Forming [$CH_2NH_2^+$ (*m*/*z* 30) + COOH], and [CH_2NH_2 + $COOH^+$ (*m*/*z* 45)]. Figure 1 shows the potential energy profile of the dissociation of the glycine cation to form [$CH_2NH_2^+$(*m*/*z* 30) + COOH], [CH_2NH_2 + $COOH^+$(*m*/*z* 45)], [$NH_2CHCOOH^+$(*m*/*z* 74) + H], [$CH_2NH_2CO^+$(*m*/*z* 58) + OH], [$CH_2NH_2^+$ + CO + OH], and [CH_2COOH^+(*m*/*z* 59) + NH_2]. Figure 2 presents the corresponding mechanisms, structures, and some geometry parameters. The structures in parentheses with double daggers represent the transition states. This formality is followed in the rest of this study except where explicitly stated. Our calculations reveal that the energy barrier of the reaction involved in abstracting COOH is 8.5 kcal/mol and that an intermediate (**HB−CO_2H**) is present in the reaction pathway between the parent cation and its fragments, [$CH_2NH_2^+$ + COOH] or [CH_2NH_2 + $COOH^+$]. This intermediate is a hydrogen-bonded complex with a short distance (1.721 Å) between the amino hydrogen in $CH_2NH_2^+$ and the oxygen in the carboxyl radical. With a formation energy that is only 1.6 kcal/mol higher than that of the parent cation, the hydrogen-bonded complex requires 14.4 kcal/mol to separate completely into [$CH_2NH_2^+$(*m*/*z* 30) + COOH] fragments and 58.7 kcal/mol, into [CH_2NH_2 + $COOH^+$(*m*/*z* 45)] fragments. Obviously, the dominant fragment is [$CH_2NH_2^+$ + COOH]; its critical energy is 16.0 kcal/mol, which is close to the experimental threshold energy of 13.9 kcal/mol.[20b] The *m*/*z* 45 signal has been suggested to be the COOH cation by Polce et al.[23] in the CAD spectrum of the glycine radical cation. The major fragmentation reaction of protonated glycine cation, $(H_3NCH_2COOH)H^+$, also yields immonium ion, $CH_2NH_2^+$, by losing CO and H_2O,[11−17] and the threshold energy of the corresponding collision-induced dissociation (CID) is 44.4 kcal/mol.[12] The theoretical study of this fragmentation mechanism has been reported by O'Hair et al.[17] and Rogalewicz et al.[16] The former found that the critical enthalpy (the minimum energy required to observe this kind of fragmentation) is 39.1 kcal/mol using the B3LYP/6-31G* method, and the latter reported that the fragmentation of lowest critical energy is 36.6 kcal/mol using the MP2(FC)/6-311+G(2d,2p)//MP2(FC)/6-31G* method with ZPVE corrected. Our results indicate that the critical energy can be as low as 16.0 kcal/mol from the glycine radical cation.

3.2 Forming [$NH_2CHCOOH^+$ (*m*/*z* 74) + H]. Removing an α-H from the glycine radical cation requires overcoming a 30.1 kcal/mol energy barrier to generate the α-glycyl radical

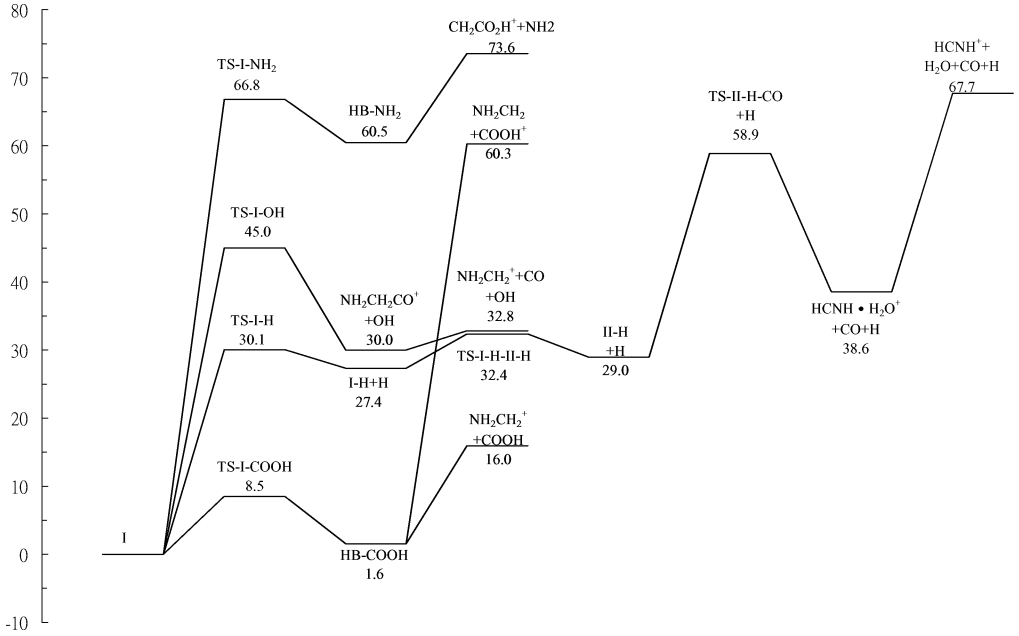

Figure 1. Potential energy profile for the fragmentation reactions of glycine cation radical (**I**) to form [$CH_2NH_2^+$ + COOH], [$NH_2CHCOOH^+$+H], [$CH_2NH_2^+$+CO&OH], [CH_2COOH^++NH_2], and [$HCNH^+$+H+CO+H_2O] using CCSD(T)//B3LYP method with 6-31+G(d,p) basis sets. Energies are in kcal/mol and are relative to glycine cation radical (**I**) conformer.

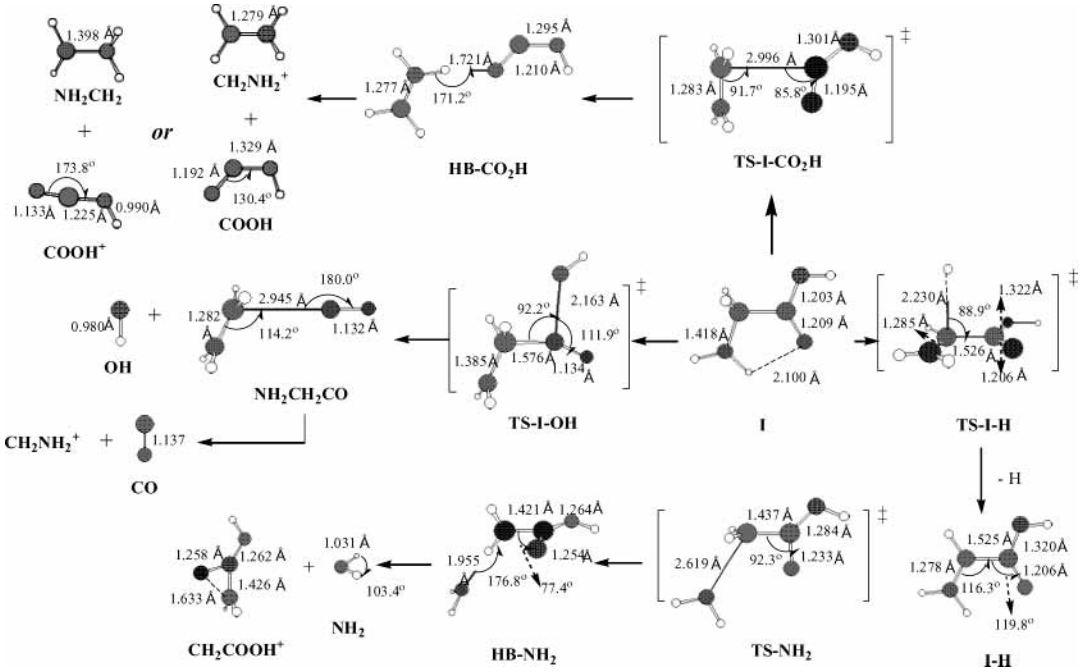

Figure 2. Mechanisms of glycine cation radical (**I**) to form [$CH_2NH_2^+$+COOH], [CH_2NH_2+$COOH^+$], [$NH_2CHCOOH^+$+H], [$CH_2NH_2^+$+CO&OH], and [CH_2COOH^++NH_2].

(**I**−**H**), which has C_s symmetry, with all atoms coplanar. This does not concur with the results calculated by Rega et al.[4] using the B3LYP/6-31G** method because that their calculated result shows that there are three H atoms ((N)H_2 and (C)H) of the glycyl radical that are out of the plane, but the geometrical parameters of our calculated result are similar to the results calculated by O'Hair et al.[9] using the MP2(FC)/6-31+G* method. The α-glycyl cation can undergo further fragmentation reactions[5−7,9] to yield **HCNH**$^+$(*m*/*z* 28) and some other fragments with low intensity. Our results show that the *m*/*z* 28 signal that was observed in ref 20 may originate the fragmentation of the glycyl cation, and we will discuss this kind of fragmentation in section 3.10.

3.3 Forming [CH_2COOH^+(*m*/*z* 59) + NH_2]. The glycine radical cation can also undergo a direct C−N bond cleavage reaction. With a 66.8 kcal/mol energy barrier, the abstraction of NH_2 from the parent cation is much more difficult than the abstraction of COOH and α-H. An intermediate (**HB**−**NH$_2$**) is also involved in the reaction pathway, with a short distance (1.955 Å) between the methyl hydrogen and the amino nitrogen. This cation−radical complex can be a hydrogen-bonded complex, which can be broken apart with 13.1 kcal/mol. The critical energy to yield $CH_2CO_2H^+$ (*m*/*z* 59) by losing NH_2 from the glycine radical cation is 73.6 kcal/mol, and the *m*/*z* 59 signal was not found in the work of Vorsa el al.[20a] but was detected by the N_FR spectra,[23] suggesting that the fragment is generated

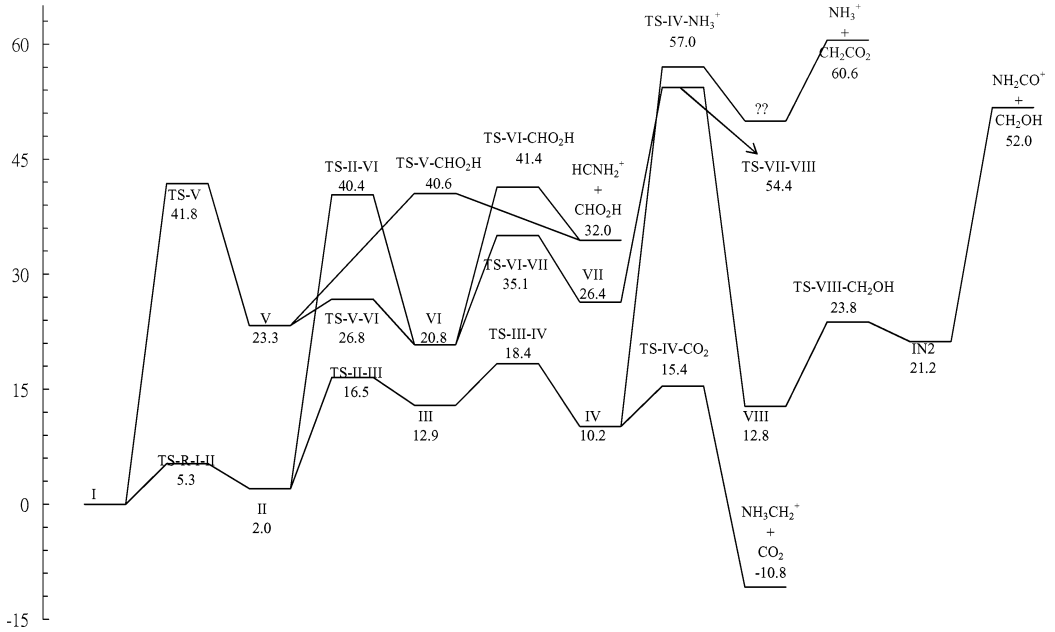

Figure 3. Potential energy diagram for the fragmentation reactions of glycine cation radical (**I**) to form $[CH_2NH_3^+ + CO_2]$, $[NH_3^+ + CH_2CO_2]$, $[NH_2CO^+ + CH_2OH]$, and $[HCNH_2^+ + CH(O)OH]$ using the CCSD(T)//B3LYP method with 6-31+G(d,p) basis sets. Energies are in kcal/mol and are relative to glycine cation radical (**I**) conformer.

by losing an O atom. The fragmentation energy of forming $[O + NH_2CH_2OH^+]$ is 141.8 kcal/mol, which is higher than the fragmentation energy of forming $[NH_2 + CH_2COOH^+]$, 75.5 kcal/mol using the (U)B3LYP/6-31+G** method with ZPVE corrected. From this result, we suggest the *m*/*z* 59 is formed by the loss of NH_2 from the glycine radical cation.

3.4 Forming $[CH_2NH_2CO^+$ (*m*/*z* 58) + OH], $[CH_2NH_2^+$ + CO + OH]. When undergoing direct C−O bond cleavage, the glycine radical cation can generate the CH_2NH_2CO cation (*m*/*z* 58) with the activation energy, 45.0 kcal/mol, to abstract the OH. This cation was detected by N_fR spectrum,[23] but no signal was found in the work of Vorsa et al.[20] We found that the fragment, $CH_2NH_2CO^+$(*m*/*z* 58), is an ion−molecule complex with a distance of 2.945 Å between the methyl hydrogen and the carbonyl carbon. It can be broken easily into $CH_2NH_2^+$ and CO, requiring only 2.8 kcal/mol of energy. Maybe, it is a reason that the signal did not appear in the high-energy mass spectrum.[20a] This type of bond breakage is similar to that observed in recent theoretical studies[13−15,17] on protonated glycine. The glycine that is protonated on the hydroxyl oxygen, $[NH_2CH_2C(O)-OH_2]^+$, also forms an ion−dipole complex, from which CO can be easily detached after the water molecule is abstracted. The bond lengthes of N−C, C−C, and C−O of the $NH_2CH_2C(O)$ cation in our calculated results are 1.282, 2.945, and 1.132 Å, respectively, and are similar to those found by Rogalewicz et al.[15] (1.28, 2.93, and 1.15 Å, respectively) using the MP2(FC)/6-31G* method. The corresponding dissociation energy reported by Rogalewicz et al.[15] is 4.1 kcal/mol, a little bit larger than our calculated result, which is 2.8 kcal/mol.

3.5 Forming $[CH_2NH_3^+$ (*m*/*z* 31) + $CO_2]$ and $[NH_3^+$ (*m*/*z* 17) + $CH_2CO_2]$. The fragmentation precursor to $[CH_2NH_3^+ + CO_2]$ and $[NH_3^+ + CH_2CO_2]$ should be conformer **IV**, which is generated by transferring the hydroxyl hydrogen to the amino nitrogen. The potential energy profile of the above fragmentation reactions from a glycine radical cation is shown in Figure 3, and Figure 4 presents the corresponding reaction mechanisms. Conformer **II** must be generated before the formation of conformer **IV,** and there are two different routes that can generat conformer **II**.

$$\left.\begin{array}{l}\text{Path 1: I} \xrightarrow{\text{TS-I-II}} \\ \text{Path 2: I} \xrightarrow{\text{TS-R-I-II}}\end{array}\right\} \text{II} \xrightarrow{\text{TS-II-III}} \text{III} \xrightarrow{\text{TS-III-IV}} \text{IV}$$

In Path 1, the hydroxyl hydrogen is transferred to the carbonyl oxygen to generate conformer **II**, but in Path 2, conformer **II** can be generated by simply rotating the C−C bond of conformer **I.** The energy barrier of Path 2 is 5.3 kcal/mol, and that of Path 1 is 45.3 kcal/mol. This newly formed hydroxyl group rotates to the other side to form **III**, and then its hydroxyl hydrogen is transferred to the amine group.

Abstracting CO_2 from conformer **IV** requires an energy barrier of 5.2 kcal/mol to generate $CH_2NH_3^+$ (*m*/*z* 31). The relative energy of **TS-IV-NH$_3$** (57.0 kcal/mol) is lower than the fragmentation energy (60.6 kcal/mol) required to abstract CH_2CO_2 from conformer **IV** to generate NH_3^+ (*m*/*z* 17). This result implies the present of an intermediate between the **TS-IV-NH$_3$** and $[NH_3^+ + CH_2CO_2]$ fragments, which we failed to identify in this study.

From the 195-nm photoionization mass spectrum[20a] and N_fR spectrum[23] of the glycine radical cation, by taking $CH_2NH_2^+$, the most abundant ion, as a reference (100%), we found *m*/*z* 31 amounts to be 13.3 and 25%, respectively. Somehow the *m*/*z* 31 signal failed to appear in MI and CAD spectra.[23] Our results indicate that the critical energy required to generate the NH_3-CH_2 and NH_2CH_2 cations is 18.4 and 16.0 kcal/mol, respectively. Found in the 195-nm photoionization mass spectrum[20a] and the CAD and NR spectra[23] of the glycine radical cation, the *m*/*z* 17 is suggested to be the OH cation by Polce et al.[23] This suggestion is supported by the detection of the *m*/*z* 18 in the CAD of perdeuteroglycine radical cation.[23] However, the intensity of *m*/*z* 20, which might be ND^{3+}, also increases from 0 to 9 if the intensity of *m*/*z* 34 is set to be 100.23. Therefore, the identity of *m*/*z* 17 still remains unsolved by the perdeuteroglycine radical cation experiment.[23] However, from our results,

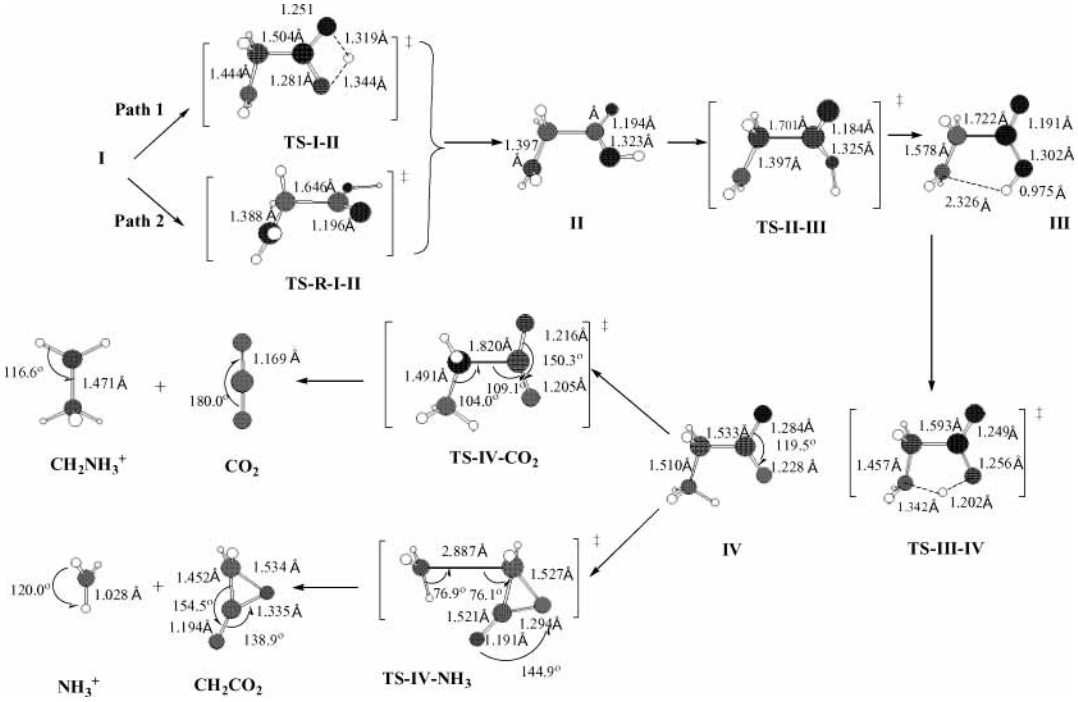

Figure 4. Mechanisms of glycine cation radical (**I**) to form $[CH_2NH_3^+ + CO_2]$ and $[NH_3^+ + CH_2CO_2]$.

all of the fragmentation energies of yielding OH^+, with various combinations of the neutral C_2NOH_4 species, are higher than that yielding NH_3^+ and CH_2CO_2 fragments. Therefore, we suggest the signal of *m*/*z* 17 should be the NH_3 cation. The intramolecular proton-transfer energy barrier and relative energy from **III** to **IV** found in ref 22 are 5.8 and 4.8 kcal/mol using CCSD(T) with D95++(d,p) basis set, and our results are 5.5 and 2.7 kcal/mol, respectively thus, it is sufficient to use CCSD-(T)//B3LYP with the 6-31+G(d,p) basis set.

3.6 Forming $[NH_2CO^+$ (*m*/*z* 44) + $CH_2OH]$ and $[HCNH_2^+$ (*m*/*z* 29) + CH(O)OH]. NH_2CO^+, with CH_2OH as the neutral counterpart, is determined herein to be probably the *m*/*z* 44 species. Generating the above fragments from the conformer **I** involves three intramolecular rearrangements; it is obtained by transferring the two α-H atoms to the carbon of the carboxyl group and by transferring the oxygen atom of the carbonyl group to the α-C. The transfer of oxygen must be preceded by the transfer of one proton and a rotation reaction because one of the two methylene hydrogens transferred to the carboxyl carbon can increase the sp3 hybridization characteristics of the carbonyl oxygen, reducing the activation energy for the oxygen transfer and because the hydroxyl hydrogen transferred to the carbonyl carbon can change the nearly coplanar geometry of the original carbonyl oxygen and amino group, which would otherwise hinder the transfer of oxygen

$$\text{Path 3: I} \xrightarrow{\Delta E_a = 41.8} \text{V} \xrightarrow{\Delta E_a = 3.5} \text{VI}$$

$$\text{Path 4: I} \xrightarrow{\Delta E_a = 5.3} \text{II} \xrightarrow{\Delta E_a = 38.4} \text{VI}$$

Thus, two different pathways, Paths 3 and 4, are identified according to the order of the two aforementioned reactions by which this oxygen transfer precursor (conformer **VI**) is formed. Path 3 refers the initial transfer the methylene hydrogen followed by a simple C−C bond rotation whereas the transfer in Path 4 is in the opposite order. Figure 5 depicts these mechanisms. Figure 3 shows the corresponding energy profile. Path 4 is the dominant reaction pathway because the critical energy and activation energy of Path 4 are lower than those of Path 3.

The energy barrier for transferring the carbonyl oxygen of conformer **VI** to the α-C, forming conformer **VII**, is 14.3 kcal/mol. When the α-H forms a three-center bond with the two carbons, the corresponding transition state (**TS-VII-VIII**) might imply that the α-H transfers to the other carbon accompanied by the oxygen transfer, resulting in the spontaneous formation of the final products, NH_2CO^+ and CH_2OH. A search of the potential surface using the intrinsic reaction coordinate (IRC) technique reveals that this is not the case, another structural rearrangement should be involved. The final structural rearrangement proceeds by a reaction from conformer **VII** to **VIII**. It involves the transfer of a proton from the proton of (C)H in the $CHNH_2$ to the hydroxyl methylene group (CHOH) and two simultaneous reactions, the breakage of the O−C bond in the $NH_2CHO-CHOH$ and the formation of a bond between the two carbon atoms. The energy barrier is 28.0 kcal/mol. The C−C bond in conformer **VIII** can be broken rather easily, requiring that an energy barrier of only 11.0 kcal/mol be overcome. A possible prefragmentation intermediate (**IN2**) is also found. Notably, conformer **IN2** is a hydrogen-bonded complex with a rather short distance (1.395 Å) between one of the two protons in the NH_2CO and the oxygen of the CH_2OH. **IN2** is more stable than its fragmentation products, NH_2CO and CH_2OH, and the energy difference is 10.7 kcal/mol.

In the fragmentation reaction between $HCNH_2^+$ and CH(O)-OH, the primary subreaction is the breakage of the C−C bond, and conformers **V** and **VI** are the probable precursors. The dominant pathway of this reaction is through conformer **V**. The energy barriers to the reaction of conformer **V** to generate the final products is lower (17.3 kcal/mol) than that of the reaction with conformer **VI** (20.6 kcal/mol). The pathway through conformer **V** has fewer steps than that through conformer **VI**. Notably, conformer **VI** is an intermediate in the formation of $[HCNH_2^+ + CH(O)OH]$ and $[NH_2CO^+ + CH_2OH]$.

3.7 Forming $[HCCN^+$(*m*/*z* 39)+2$H_2O]$. In the formation of $HCCN^+$, two amino hydrogen atoms and the two α-Hs in the conformer **I** must be transferred to another atom before two water molecules are abstracted from the cation. Figure 6 shows the corresponding energy profiles, and Figure 7 presents the

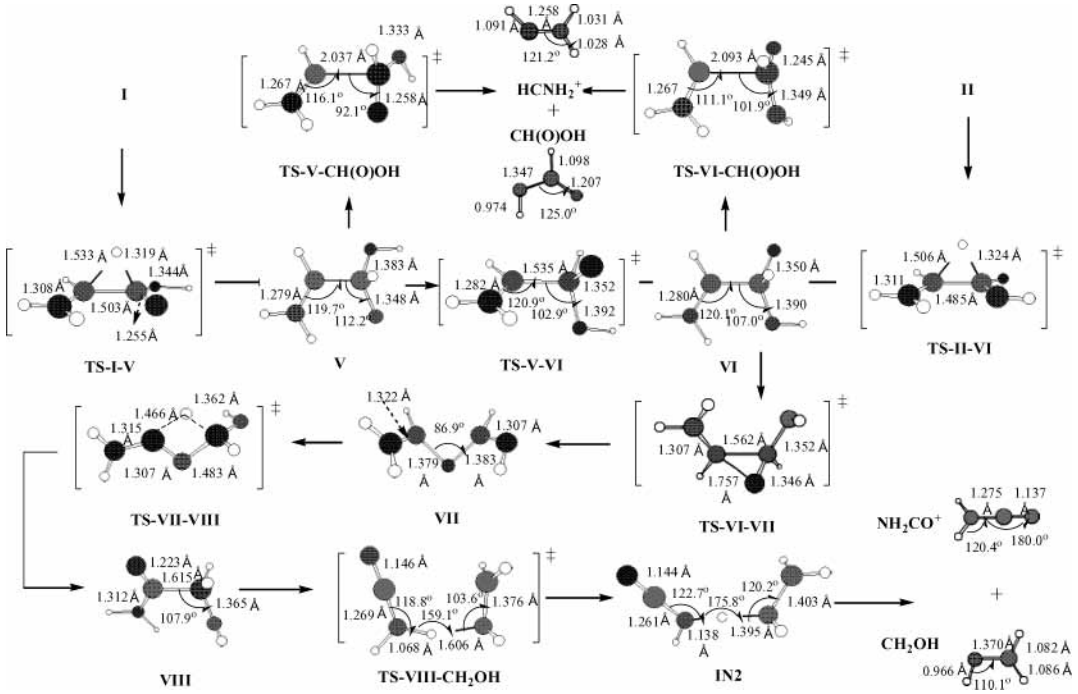

Figure 5. Mechanisms of glycine cation radical conformer **I** and **II** to form [NH_2CO^++CH_2OH] and [$HCNH_2^+$+CH(O)OH].

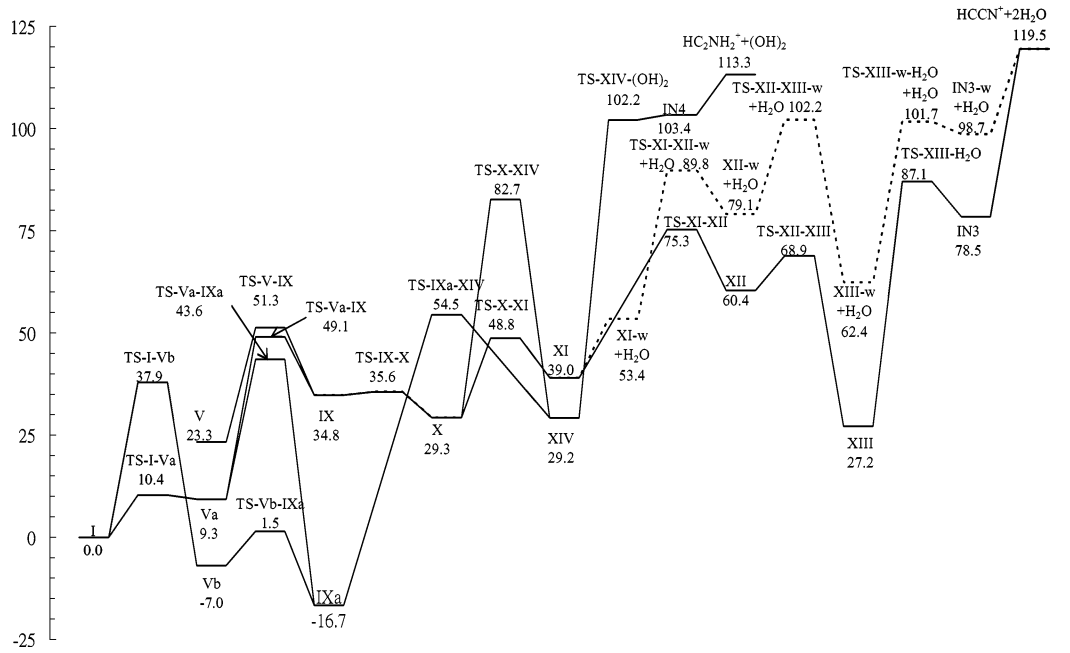

Figure 6. Potential energy diagram for the fragmentation reactions of glycine cation radical (**I**) to form [$HC_2NH_2^+$+$(OH)_2$] and [$HCCN^+$+$2H_2O$] using the CCSD(T)//B3LYP method with 6-31+G(d,p) basis sets. Energies are in kcal/mol and are relative to glycine cation radical (**I**) conformer.

probable reaction mechanisms. As shown in Figure 7, two pathways, Paths 5 and 6, describe the transfer of two hydrogen atoms, one from the amino group and the other from methylene group, both to the carbonyl group.

$$\text{Path 5: I} \xrightarrow{\Delta E_a = 41.8} \text{V} \xrightarrow{\Delta E_a = 28.0} \text{IX}$$

$$\text{Path 6: I} \xrightarrow{\Delta E_a = 10.4} \text{Va} \xrightarrow{\Delta E_a = 39.8} \text{IX}$$

The primary difference between these two pathways is the order in which the hydrogen atoms are transferred; both lead to the formation of conformer **IX**. The activated complexes suggest that Path 6 is the preferred pathway by which conformer **IX** is formed.

The third hydrogen transfer might proceed in one of two ways by either transferring a proton from the amino or the methylene group. The product of the transfer of the methylene hydrogen will have a linear H−N−C−C structure, making the last transfer of hydrogen rather difficult, that is, with high energy barriers and more reaction steps. The pathway by which hydrogen is transferred from the amino group is, in fact, favored. Hence, this study addresses only the former reaction, which requires the transfer of an amino hydrogen atom to a hydroxyl group. Conformer **XI** is formed by hydrogen transfer, and interestingly, this conformer is a cation−water complex with a short C−O distance (1.663 Å) between the cation and the water. Separating this cation−water complex requires 14.4 kcal/mol. Further reactions involve dissociating the water molecule and two proton

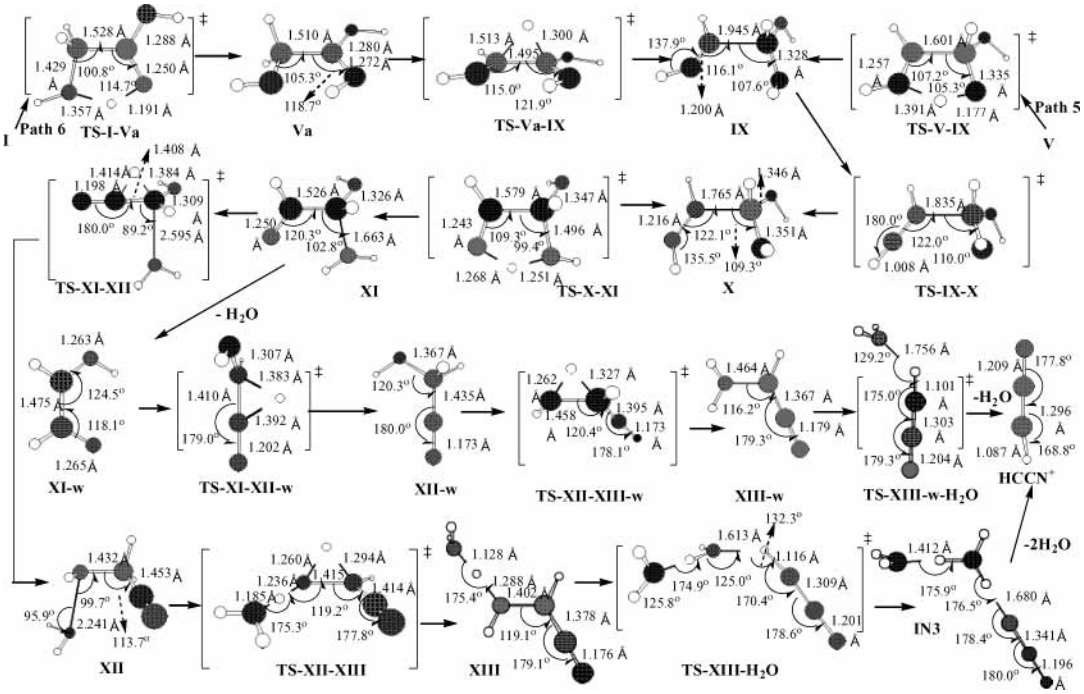

Figure 7. Mechanism of glycine cation radical conformer **I** and **V** to form $HCCN^+$ and $2H_2O$.

transfers, which are hydrogen transfers from the α-C to the carbonyl carbon and from the carbonyl carbon to the hydroxyl oxygen.

These reactions can proceed with or without (dashed line) the dissociation of the water molecule formed in the preceding step, and their reaction mechanisms are quite similar, but they have different reaction energies, which are shown in Figure 6. In the reactions of conformer **XI-w** to form **XIII-w** with the dissociation of water molecule, the corresponding energy barriers of the two proton transfers and the abstraction of another water molecule are 36.4, 23.1, and 39.3 kcal/mol, respectively. Another 20.8 kcal/mol is required to break apart the water molecule completely because an intermediate (**IN3-w**) is formed, having a very short distance (1.434 Å) between the oxygen in the water molecule and the hydrogen in the cation.

However, the energy barriers of the previous reactions with water molecule attached are 36.3, 8.5 ,and 59.9 kcal/mol, but the relative energy of the transition state complexes (TS) are lower than those without the water molecule attached. The TS of the latter are higher than the TS of the former about 14.4, 33.2, and 14.6 kcal/mol, respectively. Not only are the relative energies of the TSs low, but the energies of the corresponding intermediates are also low. Therefore, the H_2O molecules can stabilize both the reaction intermediates and the transition states. The search of the potential energy surface (near or around) **IN3**, which is an intermediate present before the cation radical is completely separated into fragments, reveals an interesting finding. **IN3** can further be broken into NC_2H^+ (*m*/*z* 39) and $(H_2O)_2$, which were detected in ref 20 but with a rather low intensity. With reference to the formation of the $HCCN^+$ cation radical, the order of proton transfer is very important, and the cation's neutral counter-water molecules may participate in reactions that stabilize activated complexes and intermediates.

3.8 Forming $[HCCNH_2^+$ (*m*/*z* 41) + $(OH)_2]$. The fragmentation precursor in the formation of $HCCNH_2^+$ can be something similar to conformer **XIV**, which is the product of two proton-transfer reactions, in which one proton is transferred to the carbonyl oxygen and the other is transferred to the carboxyl carbon to weaken the C−O bonds. The formation of conformer **XIV** involves many consecutive proton transfers as described in the preceding section. Among the possible combinations of proton-transfer sequences that generate conformer **XIV**, four pathways have energy barriers below the photodissociation energy. These are Paths 7−10. Figure 8 and Figure 6 show their mechanisms and energy profiles, respectively.

$$\text{Path 7: I} \xrightarrow{\Delta E_a = 41.8} \text{V} \xrightarrow{\Delta E_a = 28.0} \text{IX} \xrightarrow{\Delta E_a = 0.8} \text{X} \xrightarrow{\Delta E_a = 53.4} \text{XIV}$$

$$\text{Path 8: I} \xrightarrow{\Delta E_a = 10.4} \text{Va} \xrightarrow{\Delta E_a = 39.8} \text{IX} \xrightarrow{\Delta E_a = 0.8} \text{X} \xrightarrow{\Delta E_a = 53.4} \text{XIV}$$

$$\text{Path 9: I} \xrightarrow{\Delta E_a = 10.4} \text{Va} \xrightarrow{\Delta E_a = 34.3} \text{IXa} \xrightarrow{\Delta E_a = 71.2} \text{XIV}$$

$$\text{Path 10: I} \xrightarrow{\Delta E_a = 37.9} \text{Vb} \xrightarrow{\Delta E_a = 8.5} \text{IXa} \xrightarrow{\Delta E_a = 71.2} \text{XIV}$$

The critical energy (**TS-X-XIV**, 82.7 kcal/mol) of Paths 7 and 8 is higher than that of Paths 9 and 10 (**TS-IXa-XIV**, 54.5 kcal/mol). Because of the low critical energy and the fewer reaction steps involved, Paths 9 and 10 are clearly more likely reaction pathways than Paths 7 and 8. However, the rate-determining step of formation of NH_2CCH^+ is the final step, that is, to separate $(OH)_2$ from conformer **XIV**, with a corresponding energy barrier of 73.0 kcal/mol. Intrinsic reaction coordinates (IRC) are used to identify the transition state (**TS-XIV−(OH)$_2$**) in the dissociation of the $(OH)_2$ molecule from **XIV**, and **IN4** is observed. Notably, the relative energy of **IN4** is lower than that of **TS-XIV−(OH)$_2$**, as determined by B3LYP level, but the single point energy calculated using the CCSD(T) level is around 1.2 kcal/mol higher than the energy of this transition state.

It is interesting that the *m*/*z* 41 HC_2NH_2 cation is generated through **IXa,** which is one of the fragments of the glycine radical cation in the enol form, with the same structure as **1a** found by Marino and Russo,[24] and the *m*/*z* 41 also has been observed in NR spectrum, which indicates that the HC_2NH_2 cation may be generated through the enol form of the glycine radical cation. It requires a critical energy of 54.6 kcal/mol (the energy difference of **IXa** and **TS-I-Va**) from **IXa** to **I,** and it shows

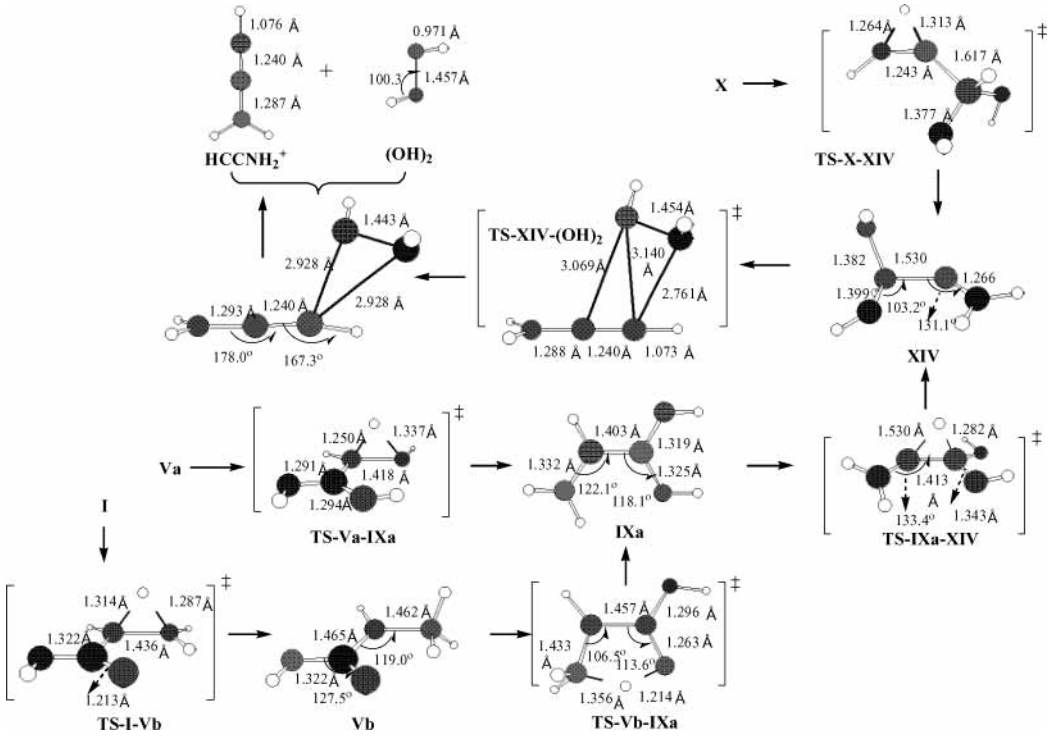

Figure 8. Mechanism of glycine cation radical conformer **I**, **Va**, and **X** to form $HC_2NH_2^+$ and H_2O_2.

that the enol form of the glycine radical cation is difficult to isomerize to the keto form. Therefore, one can observe the different patterns of mass spectra between the enol and keto forms of the glycine cation radical. It is consistent with the results found by Polce and Wesdemiotis.[23] The previous studies[23,24] also indicate that the enol form of the glycine cation radical favors losing water and generating an aminoketene radical cation, but there is no meaningful signal of *m*/*z* 41 observed in the spectrum of study of Vorsa et al.[20a]

3.9 Forming [$HCNH^+$ (*m*/*z* 28) + CHO + H_2O] and [$HCNH^+$ (*m*/*z* 28) + $CH(OH)_2$]. The formation of $HCNH^+$, CHO, and H_2O from conformer **I** requires at least the transfer of two protons into the carboxyl acid group, that is, one from the amine group and the other from the methylene group, as well as the breakage of the C−C bond. This fragmentation reaction includes the detachment of a single water molecule, therefore, the reaction pathways can be differentiated by whether the cation−water complex is generated during the overall reaction. As explained in section 3.7, the water molecule can stabilize both the transition states and the intermediates by generating a cation−water complex. Only those pathways that involve cation−water complex are considered below. Searching all types of the order of the proton transfers shows two reaction pathways with lower energies. They are Paths 11 and 12.

$$\text{Path 11: V} \xrightarrow{\Delta E_a = 52.7} \text{XVI} \xrightarrow{\Delta E_a = 53.4} \text{XVII} \xrightarrow{\Delta E_a = 10.5} \text{IN5}$$

$$\text{Path 12: Va} \xrightarrow{\Delta E_a = 53.4} \text{XVIa} \xrightarrow{\Delta E_a = 47.7} \text{XVIIa} \xrightarrow{\Delta E_a = \text{little}} \text{IN5a}$$

Figures 9 and 10 present their energy profiles and corresponding mechanisms, respectively. These two pathways have many shared features. First, they involve the transfer of three protons, two of which precede the formation of the cation−water complex. Second, the C−C bond breaks immediately following the final proton transfer and involves a high energy barrier. Third, an intermediate is formed before the CHO fragment detaches. Despite these commonalities, the details of these two pathways differ considerably; for example, in Path 11, the first two proton transfers are all from the methylene group to the carbonyl group and the final proton transfer is from the amine group to the original α-C. However, in Path 12, the first proton is transferred from the amine group to the carbonyl group, the second is transferred from the methylene group to the carbonyl group, and the last is transferred from the hydroxyl group to the original carbonyl carbon to generate the CHO group. Apart from the differences associated with the transfers of protons, the primary difference between these two pathways is in the structure of the cation−water complex formed. In Path 11, the water molecule is near the proton in the CHO group, but in Path 12, the water molecule moves from the CHO side toward the HCNH side. Notably, this motion stabilizes the transition state in the CHO detachment because HCNH exhibits more cation characteristics than CHO. The total electronic energy of **TS-XIIa-CHO** is below that of its reaction precursor (**XIIa**), but that of **XIIa** is 1 kcal/mol higher than that of **TS-XIIa-CHO** just after ZPVE correction. Two intermediate species, **IN5** and **IN5a**, are also found during the abstraction of the CHO radical, but somehow, the CHO radical does not separate completely. The dominate mechanism to $HCNH^+$, CHO, and H_2O is Path 11 because the critical energy is lower than it is in Path 12.

The precursor of the formation of $HCNH^+$ and $CH(OH)_2$ should be conformer **IX.** From the fact that the bond length of C−C of **IX** is 1.945 Å, the fragmentation of **IX** to form $HCNH^+$ and $CH(OH)_2$ fragments is rather easy. The energy profile and mechanism are presented in Figure 9 and Figure 11, respectively. The energy barrier of this reaction is only 3.3 kcal/mol, and there exists an intermediate (**IN6**). Unfortunately, the H atom that also can transfer from the hydroxyl group to the NH group is following the breakage of C−C bond in **IX**. We found that N and O of **IN6** share this H atom, but the distance of N···H (1.101 Å) is shorter than the distance of O···H (1.486 Å). The energy requirement of **IN6** to form the fragments of [$HCNH^+$ and $CH(OH)_2$] and [$HCNH_2^+$ and CH(O)OH] are 44.3 and 18.2

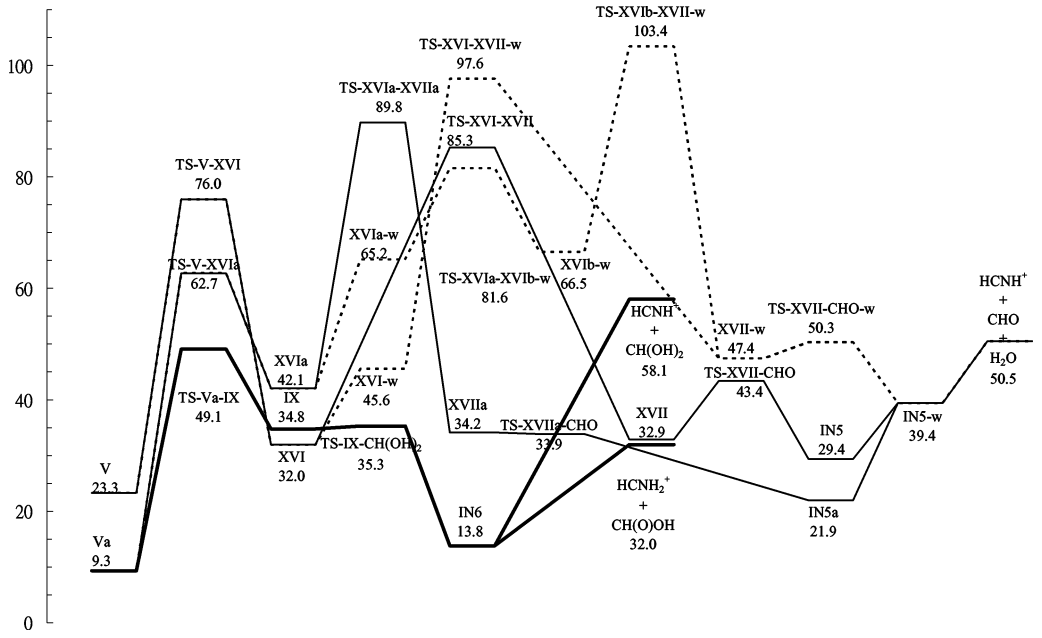

Figure 9. Potential energy diagram for the fragmentation reactions of glycine cation radical conformer **V** and **Va** to form [$HCNH^+$, CHO and H_2O], [$HCNH^+$ and $CH(OH)_2$], and [$HCNH_2^+$ and CH(O)OH] using the CCSD(T)//B3LYP method with 6-31+G(d,p) basis sets. Energies are in kcal/mol and are relative to glycine cation radical (**I**) conformer.

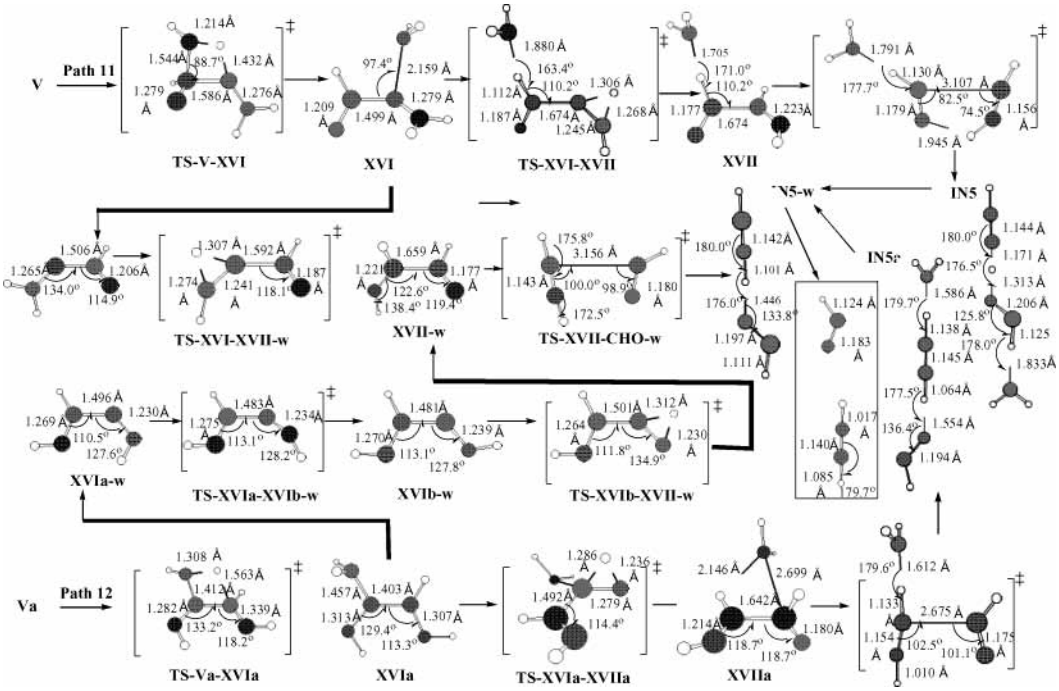

Figure 10. Mechanisms of glycine cation radical conformer **V** and **Va** to form $HCNH^+$, CHO, and H_2O.

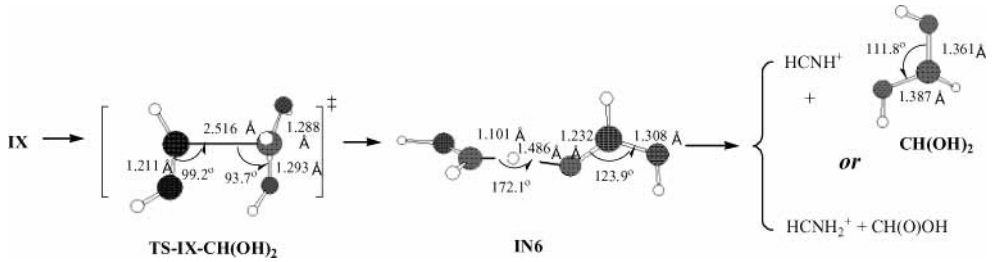

Figure 11. Mechanisms of glycine cation radical conformer **IX** to form $HCNH^+$, $CH(OH)_2$ and $HCNH_2^+$, and CH(O)OH.

kcal/mol, respectively. It is evident that the dominant fragments are $HCNH_2^+$ and CH(O)OH from **IN6**, but it can probably apply a low energy channel to yield $HCNH^+$ and $CH(OH)_2$ fragments. The critical energy of forming $HCNH^+$ and $CH(OH)_2$ fragments is 58.1 kcal/mol, lower than that of forming $HCNH^+$, CHO, and H_2O fragments from **I** (85.3 kcal/mol), although the

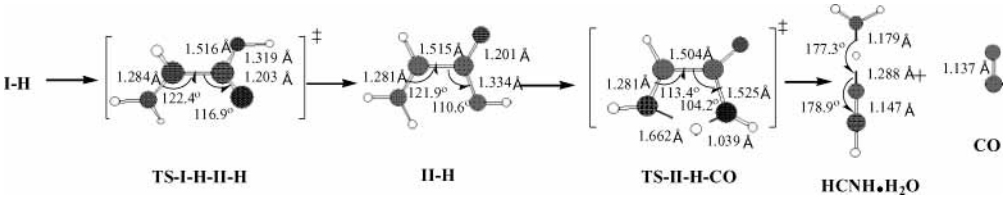

Figure 12. Mechanism of glycyl cation (**I**−**H**) to form $HCNH^+$, CO and H_2O.

TABLE 2: Summary of the Fragment Cation Species along with Their Corresponding Neutral Species, Critical Energies, and the Relative Intensity of the Signals Observed in Experiment[20]

m/*z*	fragment ion	corresponding neutral species	critical energies[a]	observed intensity[b]
30	$NH_2CH_2^+$	COOH	16.0	100
31	$NH_3CH_2^+$	CO_2	18.4	13.3
74	$NH_2CHCO_2H^+$	H	30.1	4
29	$HCNH_2^+$	CHO_2H	41.8	4
44	NH_2CO^+	CH_2OH	54.4	6.7
28	$HCNH^+$	$CH(OH)_2$	58.1	4
17	NH_3^+	CH_2CO_2	60.6	4
45[c]	$COOH^+$	NH_2CH_2	62.3	
28	$HCNH^+$	$CO+H_2O$	67.7	4
28	$HCNH^+$	$CHO + H_2O$	85.3	4
59[d]	$CH_2CO_2H^+$	NH_2	73.6	
41	$HC_2NH_2^+$	$(OH)_2$	113.3	4
39	$HCCN^+$	$(H_2O)_2$	115.7	4

[a] The critical energy is defined as the minimum energy needed to observe the particular fragmentation, as described in ref 16. [b] The relative intensity of signals reported in ref 20, by setting intensity of *m*/*z* 30 as 100. [c] This signal is not observed in ref 20 but appears in CAD and NR MS experiments in ref 23. [d] The *m*/*z* 59 signal was not found in the work of Vorsa el al. in ref 20 but was detected by the N_fR spectra in ref 23.

fragmentation energy of the former is higher than the fragmentation energy of the latter. It is because that, in the latter fragmentation, there is a high-energy barrier between **XVI** and **XVII** in the reaction mechanism**.**

3.10 Forming [$HCNH^+$ (*m*/*z* 28) + CO + H_2O] from the Glycyl Radical. The formation of $HCNH^+$ from conformer **I** requires at least 85.3 kcal/mol, higher than the internal energy of 83 kcal/mol[20] (the rest of the energy after absorbing two 195-nm photons and ionizing one electron (the IP of glycine is 8.8 eV)). The main peak of the glycyl radical is *m*/*z* 28,[5−7] and our study also indicates that it is easy to abstract the hydrogen atom. Apart from the mechanism suggested in Scheme 2 of Polce and Wesdemiotis,[5] our results indicate that the first step is to rotate C−C bond to form **II**−**H**, CO is then abstracted, and the $HCNH{\cdot}H_2O$ complex is formed with the hydrogen of NH_2 group interacting with hydroxyl group. Excluding H_2O from the $HCNH{\cdot}H_2O$ complex requires 29.1 kcal/mol. Although we thought that there was an intermediate before forming [HCNH_H_2O+CO], we failed to determine this intermediate. The potential energy profile has been shown in Figure 1, and the corresponding mechanism is presented in Figure 12. Our results imply that the HCNH (*m*/*z* 28) cation can be formed from the refragmentation of the glycyl radical. The relative energy of $HCNH^+$, H_2O, and CO fragments with respect to that of the glycyl cation is 40.3 kcal/mol, which is close to the 41.8 kcal/mol found in ref 6 using the G2(MP2) method. It also indicates that the CCSD(T)/6-31+G**//B3LYP/6-31+G** with ZPVE corrected method is sufficient to estimate the fragmentation energies of the glycine cation radical.

4. Conclusions

The criterion of low fragmentation energy has been applied to find the possible fragments of the glycine radical cation, and the *m*/*z* = 17, 28, 29, 30, 31, 39, 41, 44, 45, 59, and 74 peaks are proposed to result from NH_3^+, $HNCH^+$, H_2NCH^+, $NH_2CH_2^+$, $H_3NCH_2^+$, $NCCH^+$, H_2NCCH^+, NH_2CO^+, $COOH^+$, $CH_2CO_2H^+$, and $NH_2CHCO_2H^+$, respectively. Their corresponding critical energy requirements are 60.6, 58.1, 41.8, 16.0, 18.4, 115.7, 113.3, 54.4, 60.6, 73.6, and 30.1 in kcal/mol, respectively. The formation of the $NCCH^+$ and H_2NCCH^+ fragments requires very high energy, suggesting that other fragmental components can be involved. The obtained results indicate that the dominant fragmentation process is the cleavage of C_α−C by abstracting COOH, corresponding to the *m*/*z* 30 peak ($NH_2CH_2^+$), which is consistent with experimental observations. Interestingly, the *m*/*z* 59 peak does not appear in the experiment. The neutral species of *m*/*z* 28 ($HCNH^+$) peak is $CH(OH)_2$ rather than [CHO + H_2O] because the corresponding critical energy of the latter is higher than that of the former. The signal of *m*/*z* 28 may originate from the fragmentation of the glycyl radical. The water molecule is also found to participate in stabilizing the intermediates and transition states in some fragmentation processes, such as the formation of $HCCN^+$ and $HCNH^+$ fragments. Thirteen different fragmentation conformers of the glycine radical cation are identified. Among all of them, the **IXa** conformer, $NH_2CHC(OH)_2$, is the most stable one because its unpaired electron is shared between two carbon atoms. Seven cation−H_2O complexes (**XI**, **XII**, **XIII**, **XVI**, **XVIa**, **XVII**, and **XVIIa)** are found. Two of them (**XVIa** and **XI**) use the oxygen atom of water to bind to the α-C. **XIII** has the lowest energy of all of the cation−H_2O complexes. Eight intermediates (**HB**−$\mathbf{NH_2}$, **HB**−$\mathbf{CO_2H}$, **IN2, IN3, IN4**, **IN5a**, **IN5b**, and **IN6)** were found before the glycine cation radical is completely fragmented. Of these, **IN5** and **IN5a**, differ in the positions at which water is bound; the water is found to favor bonding to the side with more cationic character. Four cation−neutral complexes (**HB**−$\mathbf{NH_2}$, **HB**−$\mathbf{CO_2H}$, **IN2**, and **IN4)** were identified**.** Most of them require >10 kcal/mol to completely separate their cationic component from their neutral parts.

On the basis of the experimental results of Vorsa et al.,[20a] we presented the probable fragmentation reaction mechanisms

of the glycine radical cation in the keto form. Except *m*/*z* 30, the intensities of the other channels are rather small. Our calculated results are summarized in Table 2 with comparison to the experimental findings. The reaction network and the activated energies of the related fragmentation reaction can be considered to determine the distribution of the fragments and the relative intensities of the peaks observed in related mass spectrum experiments. Soon, we will use the RRKM theory with the information obtained in this study to estimate the intensity of related fragments.

Acknowledgment. We thank the National Science Council and Academia Sinica for financial support. The NCHC and the computer center of Academia Sinica are acknowledged for providing computational resources. We gratefully thank Dr. M. Hayashi for discussion and suggestion.

References and Notes

(1) (a) Stadtman, E. R. *Annu. Rev. Biochem.* **1993**, *62*, 797. (b) Stubbe, J.; van der Donk, W. A. *Chem. Rev.* **1998**, *98*, 705.

(2) Barone, V.; Adamo, C.; Grand, A.; Jolibois, F.; Brunel, Y.; Subra, R. *J. Am. Chem. Soc*. **1995**, *117*, 12618.

(3) Barone, V.; Adamo, C.; Grand, A.; Subra, R. *Chem. Phys. Lett.* **1995**, *242*, 351.

(4) Rega, N., Cossi, M.; Barone, V. *J. Am. Chem. Soc.* **1997**, *119*, 12962.

(5) Polce, M. J.; Wesdemiotis, C. *J. Am. Soc. Mass Spectrom.* **1999**, *10*, 1241.

(6) Tureček, F.; Carpenter, F. H.; Polce, M. J.; Wesdemiotis, C. *J. Am. Chem. Soc.* **1999**, *121*, 7955.

(7) Tureček, F.; Carpenter, F. H. *J. Chem. Soc., Perkin Trans. 2*, **1999**, 2315.

(8) Rega, N.; Cossi, M.; Barone, V. *J. Am. Chem. Soc.* **1998**, *120*, 5723.

(9) O'Hair, R. A. J.; Blanksby, S.; Styles, M.; Bowie, J. H. *Int. J. Mass Spectrom.* **1999**, *182/183*, 203.

(10) (a) Yu, D.; Pauk, A.; Armstrong, D. A. *J. Am. Chem. Soc.* **1995**, *117*, 1789. (b) Rauk, A.; Armstrong, D. A.; Fairlie, D. P. *J. Am. Chem. Soc.* **2000**, *122*, 9761.

(11) Beranová, S.; Cai, J.; Wesdemiotis, C. *J. Am. Chem. Soc*. **1995**, *117*, 9492.

(12) Klassen, J. S.; Kebarle, P. *J. Am. Chem. Soc*. **1997**, *119*, 6552.

(13) Bouchonnet, S.; Hoppilliard, Y. *Org. Mass. Spectrom.* **1992**, *27*, 71.

(14) Uggerud, E. *Theor. Chim. Acta*, **1997**, *97*, 313.

(15) Rogalewicz, F.; Hoppilliard, Y. *Int. J. Mass Spectrom.* **2000**, *199*, 235.

(16) Rogalewicz, F.; Hoppilliard, Y.; Ohanessian, G. *Int. J. Mass Spectrom.* **2000**, *195/196*, 565.

(17) O'Hair, R. A. J.; Broughton, P. S.; Styles, M. L.; Frink, B. T.; Hadad, C. M., *J. Am. Soc. Mass Spectrom.* **2000**, *11*, 687.

(18) Balta, B.; Basma, M.; Aviyento, V.; Zhu, C.; Lifshitz, C. *Int. J. Mass Spectrom.* **2000**, *201*, 69.

(19) Depke, G.; Heinrich, N.; Schwarz, H. *Int. J. Mass Spectrom. Ion Processes* **1984**, *62*, 99.

(20) (a) Vorsa, V.; Kono, T.; Willey, K. F.; Winograd, N. *J. Phys. Chem. B* **1999**, *103*, 7889. (b) Junk, G.; Svec, H. *J. Am. Chem. Soc.* **1963**, *85*, 839.

(21) Ban, F.; Gauld, J. W.; Boyd, R. J. *J. Phys. Chem. A* **2000**, *104*, 5080.

(22) Rodríguez-Santiago, L.; Soduoe, M.; Oliva, A.; Bertran, J. *J. Phys. Chem. A* **2000**, *104*, 1256.

(23) Polce, M. J.; Wesdemiotis, C. *J. Mass. Spectrom.* **2000**, *35*, 251.

(24) Marino, T.; Russo, N. *Rapid Commun. Mass Spectrom.* **2001**, *15*, 541.

(25) Simon, S.; Sodupe, M.; Bertran, J. *J. Phys. Chem. A* **2002**, *106*, 5697.

(26) Lu, H. F.; Li, F. Y.; Lin, S. H. *J. Chin. Chem. Soc.* **2003**, *50*, 729.

(27) Frey, M.; Rothe, M.; Wagner, A. F. V.; Knappe, J. *J. Biol. Chem.* **1994**, *269*, 12432.

(28) Parast, C. V.; Wong, K. K.; Lewisch, S. A.; Kozarich, J. W. *Biochemistry* **1995**, *34*, 2393.

(29) Sun, X.; Harder, J.; Kronk, M.; Sjoberg, B.-M.; Reichard, P. *Proc. Natl. Acad. Sci. U.S.A.* **1995**, *90*, 577.

(30) Sun, X.; Eliasson, R.; Pontis, E.; Anderson, J.; Buist, G.; Sjoberg, B.-M.; Reichard, P. *J. Biol. Chem.* **1995**, *270*, 2443.

(31) Sun, X.; Ollagnier, S.; Schmidt, P. P.; Atta, M.; Mulliez, E.; Lepape, L.; Eliasson, R.; Graslund, A.; Fontecave, M.; Reichard, P.; Sjoberg, B.-M. *J. Biol. Chem.* **1996**, *271*, 6827.

(32) Young, P.; Ohmam, M.; Sjoberg, B.-M. *J. Biol. Chem.* **1994**, *269*, 27815.

(33) Young, P.; Andersson, J.; Sahlin, M.; Sjoberg, B.-M. *J. Biol. Chem.* **1996**, *271*, 20770.

(34) The fragments of $[NH_2CH_2COOH]^+$ (**I**), $[NH_2CHCOOH]^+$ (**I**−**H**), $[CH_2COOH]^+$, $[NH_2]$, $[NH_2CH_2]^+$, [COOH], $[NH_2CH_2]$, and $[CO_2]^+$ in our calculated results are similar to those fragments found in ref 25. The conformer **IXa** in our study is similar to the conformer **1a** in ref 24, and the differences in bond length and bond angle between these two studies are within 0.01 Å and 2°, respectively.

(35) Frisch, M. J.; Trucks, G. W.; Schlegel, H. B.; Scuseria, G. E.; Robb, M. A.; Cheeseman, J. R.; Zakrzewski, V. G.; Montgomery, J. A., Jr.; Stratmann, R. E.; Burant, J. C.; Dapprich, S.; Millam, J. M.; Daniels, A. D.; Kudin, K. N.; Strain, M. C.; Farkas, O.; Tomasi, J.; Barone, V.; Cossi, M.; Cammi, R.; Mennucci, B.; Pomelli, C.; Adamo, C.; Clifford, S.; Ochterski, J.; Petersson, G. A.; Ayala, P. Y.; Cui, Q.; Morokuma, K.; Malick, D. K.; Rabuck, A. D.; Raghavachari, K.; Foresman, J. B.; Cioslowski, J.; Ortiz, J. V.; Stefanov, B. B.; Liu, G.; Liashenko, A.; Piskorz, P.; Komaromi, I.; Gomperts, R.; Martin, R. L.; Fox, D. J.; Keith, T.; Al-Laham, M. A.; Peng, C. Y.; Nanayakkara, A.; Gonzalez, C.; Challacombe, M.; Gill, P. M. W.; Johnson, B. G.; Chen, W.; Wong, M. W.; Andres, J. L.; Head-Gordon, M.; Replogle, E. S.; Pople, J. A. *Gaussian 98*, revision x.x; Gaussian, Inc.: Pittsburgh, PA, 1998.